CERN/SPSLC 94-5
SPSLC/M 531
06.01.1994

Interim Report on PS205 Run 1993

First investigation of metastable states in antiprotonic helium atoms by laser spectroscopy

PS205 Collaboration

F. E. Maas[1], R. S. Hayano, H. A. Torii
Department of Physics, University of Tokyo, 7-3-1 Hongo, Bunkyo-ku, Tokyo 113, Japan

T. Yamazaki[2], E. Widmann[3], H. Masuda, I. Sugai
Institute for Nuclear Study, University of Tokyo, 3-2-1 Midori-cho, Tanashi, Tokyo 188, Japan

N. Morita, M. Kumakura
Institute for Molecular Science, Myodaiji, Okazaki 444, Japan

F. J. Hartmann, H. Daniel, T. von Egidy, B. Ketzer, W. Müller, W. Schmid
Physik-Department, Technische Universität München, D-85747 Garching, Germany

D. Horváth
KFKI Research Institute for Particle and Nuclear Physics
H-1525 Budapest, Hungary

J. Eades
CERN, CH-1211 Geneva 23, Switzerland

[1]Inoue-foundation postdoctoral fellow
[2]spokesperson
[3]Present address: CERN, CH-1211 Geneva 23, Switzerland

1 INTRODUCTION

Following the discovery of antiproton trapping in liquid helium at KEK in 1991 [1], experiment PS205 had two runs at LEAR in November 1991 and in October/November 1992 establishing and investigating the metastable states of the neutral $\overline{p}He^+$atom in different phases of ^3He and ^4He including the effects of impurities. The results of these two runs have been reported [2, 3, 4, 5, 7] . In 1993 we challenged a laser experiment on the metastable states of the $\overline{p}He^+$atom (see also [6, 8]. The present report describes the preliminary results of our beam time in October/November 1993. Parts of the results have been submitted to publication (see preprint attached). All other results presented here are preliminary since the analysis of the data and the evaluation of the results are still under progress. Section 2 describes the high efficiency $\overline{p}$ -annihilation detection system, the gas target and the laser system. Section 3 describes the experiments performed together with first results.

2 Experimental setup

In 1993 we used the $\overline{p}$ beam from LEAR at a momentum of 200 MeV/c as a parasitic user in continuous extraction mode. From the analysis of our data taken in 1991 and 1992 we know that a fraction of 3% of the $\overline{p}$ stopped in helium are captured in metastable states of the $\overline{p}He^+$atom with lifetimes on the order of μs . The high laser light power required to induce any laser resonance annihilation of the metastable states is best achieved with a pulsed laser system which can be triggered at a random but nevertheless limited rate (400 Hz maximum). Hence it was necessary to develop a detection system with high efficiency for fast and online detection of prompt annihilations which serves as a veto to avoid spurious triggering of the laser. That is the main difference to the detection system employed in the 1991/1992 runs. Another reason for the high efficiency required is the fact that the largest fraction of annihilation products consist of charged pions which decay into muons and then into electrons. Decay electrons from the π^+ - μ^+ - e^+ decay chain for which no pion has been detected would introduce a 2.2 μs lifetime exponential background in the annihilation time spectra.

2.1 Detection system

The setup employed is shown in fig. 1. The helium gas target (see section **2.2**) is surrounded by seven so called "shower counters" labeled S. Each shower counter consists of interleaved plastic scintillators and lead plates. They can detect the charged particles released from the annihilation (mostly π^+/π^-) and also absorb high energetic photons from short-lived neutral annihilation products (mostly π^0) with 5 radiation lengths and detect the electromagnetic showers released by the photons. The "shower counters" have been tested at INS in Tokyo. The whole system of the seven counters covers a solid angle of 63% and has an efficiency of 99.7% to detect any annihilation. The antiprotons coming from the C1 beam line at LEAR have been counted in a 0.5 mm plastic scintillation counter (label B in fig. 1) which is read out in two ways.

The light from the edges is detected by two photomultiplier tubes to get a fast timing signal. From the single and coincident count rate of the tubes we can tell that the B counter has 99.9% efficiency for detecting antiprotons. A high efficiency is here also necessary since any undetected $\overline{p}$ will also introduce background in the annihilation time spectra. The light emerging from the surface of the B counter was imaged by an image-intensified CCD camera. An integration time of the CCD of about 1 s was sufficient to monitor the beam position with the camera in order to ensure the $\overline{p}$ - beam and laser beam overlap. An additional ring-shaped anticounter (label A in fig. 1) of 40 mm outer diameter and 10 mm inner diameter (thickness 1 mm) was used to veto antiprotons in the beam halo which would end at a stopping position outside of the laser beam.

2.2 Gas target

The closed system gas target was inside a liquid helium cryostat (see fig. 1) which is the same as the one employed in 1992 (see [3, 4, 5]). We had a stabilized temperature in the region from 4 K up to room temperature, the pressure was limited to 1.5 bar due to the additional quartz window for the laser light. Using a mass spectrometer and all-bakeable vacuum parts we could control the remaining impurities to be less than 1 ppm by pumping the target vessel down to below 10^{-5} mbar before filling 99.9999 % pure helium. The antiprotons entered the target vessel after slowing down in a degrader through a 0.407 mm stainless steel window. The degrader was adjusted to get a stopping position close to the entrance window to minimize multiple scattering in the helium target and get a high overlap between the laser beam and the particle beam. The heating power of the laser light has been largely reduced by the highly polished and aluminum coated stainless steel window. Details of the cryostat employed to generate the low temperatures are described in [3, 4].

2.3 Laser system

The laser system consisted of two identical systems involving four lasers in total. The reason for that is in the large uncertainties inherent in the theoretical calculations, the two laser systems helped in reducing the scan time, there were also scenarios (depending on the unknown initial population of the metastable states), in which it would have been necessary to employ a double resonance experiment in order to be able to detect any transition. Two XeCl excimer lasers (working at $\lambda = 308$ nm, Lambda Physik LPX240i) served as a pump light source for the dye solutions of the two dye lasers (Lambda Physik LPD3002). One dye laser produces an output pulse of about 30 ns length, the output power depending strongly on the efficiency, the lifetime and the age of the dye. The dye lasers were used in a broadband mode without intracavity etalon, several resonator modes are oscillating, yielding a maximum possible bandwidth of 0.007 nm at around $\lambda = 597$ nm wavelength. The frequency of the laser output radiation was constantly monitored for each dye laser separately by two wavemeters (Burleigh WA4500). In the wavemeter the transmission fringes of the laser radiation from a Fabry-Perrot interferometer have been compared with

the transmission fringes of a built-in stabilized HeNe laser. The calibration of the wavemeter has been checked once a week employing a secondary frequency standard, namely calibrated absorption lines in an argon discharge tube using the opto-galvanic effect. The gap in frequency between the calibrated argon lines and the built-in HeNe laser has been measured using a fixed space air-gap interferometer. The Laser beam had been enlarged to about 15 mm in diameter and covered the stopping distribution of the $\overline{p}$ -beam.

The two identical laser systems were specially modified for high output power and high repetition rate. To keep this state of the art laser system running is rather extensive and defined the time during which we could use the laser. The dye molecules in the dye solution of the laser are subject to decay due to absorption of UV-photons from the excimer pump laser light and have a certain lifetime which is determined by the accumulated pumping light power of the excimer laser output. Therefore we had to exchange the dye solution of the dye laser and clean the dye reservoir and the cuvettes very carefully, because even a small amount of old, cracked dye in the fresh solution acts as a catalysator for cracking dye molecules. The act of changing the dye solution takes about two hours per laser while we have to flash the dye solution reservoirs several times with clean solvent. This involves also the handling of toxic solvents and (sometimes very toxic) laser dyes. During the scanning of the laser we had to change the laser dyes about two times per day for maintaining the high dye laser output power needed.

Besides the dye laser, the excimer pumping laser itself needed cleaning of its end mirror and output coupler once per day. The output power of the pumping laser defines the output power of the dye laser, furthermore some of the dyes employed (for example DCM) have a narrow emission profile. If the frequency of the dye laser is set to the wings of this profile, the dye output power decreases by a few orders of magnitude if the excimer laser power is below a certain threshold. The excimer cleaning involved evacuating of the aggressive gas filling of the excimer gas reservoir through a special filter system and multiply flashing with inert gas before we could open the reservoir and take the mirrors out for cleaning. After inserting the mirrors into the excimer careful alignment of the mirrors with respect to the excimer laser axis using a HeNe laser is necessary. The whole process takes about three hours per laser. If during the cleaning process the alignment of the excimer laser with respect to the dye laser changed, some 20 optical elements had to be realigned.

The mirrors necessary to guide the laser beam to the apparatus are high reflectivity dielectric layer mirrors which are matched to a certain frequency region. Changing the laser dye to a different kind which covers a different frequency interval means also to change the optical elements for the appropriate frequency region. This procedure takes about 5 hours.

3 Measurements

The measurements we could perform during our limited beam time had three different accents, the experiment searching for a resonant laser induced annihilation (and investigating that resonance), the experiment on the influence of hydrogen impurities

on the metastable states (using also the laser), and further investigations on the isotope effect comparing the delayed annihilation in ^{3}He , ^{4}He , and mixtures of both (without laser) (see fig. 2 and fig. 3.)

3.1 Laser-induced resonant annihilation in metastable antiprotonic helium atoms

The principle of the laser spectroscopy of the metastable states relies on the fact that theoretical calculations of the $\overline{p}He^+$atom show that there is a sharp boarder in the lifetime of the metastable states at $\ell = 35$. For ℓ above of that value, the lifetime of the states is determined by slow radiative decay (lifetimes on the order of μs). The energy of the transitions is not sufficient to ionize the system by emitting the electron via Auger transitions. For states with ℓ below that value, the transition energy is high enough to allow Auger transitions by emitting the electron for which the expected lifetime is of the order of ns. The principle is described in detail elsewhere [8, 6]. The theoretical predictions concerning the initial population of the metastable states, the Auger lifetime, the dipole matrix elements, and the transition energy have large uncertainties, we had to prepare different types of laser dye to cover a wide frequency range. The width and height of the resonance we were looking for was also not precisely known.

The laser has been fired for every $\overline{p}$ detected by the B counter (vetoed by signals from the A counter) where no prompt annihilation within 100 ns after arrival of the $\overline{p}$ has been found. The excimer laser has an intrinsic delay of about 1.4 μs so that the light output of the dye laser enters the target at 1.8μs after the $\overline{p}$. Every event where a second $\overline{p}$ entered the target within a 10 μs time window has been discarded in the analysis (post pileup rejection). Any pre pileup has been rejected in the hardware electronics.

The search for any resonance signal was done by scanning both lasers in different wavelength regions. Before we have found a signal both signal strength and width of the resonance line were not very well known. Therefore we scanned the frequency with a step size equal to the laser bandwidth. A run at one frequency point took a mean time of 20 minutes. At a laser wavelength of $\lambda = 597.26$ nm we found a sharp peak in the annihilation time spectrum, for details, see attached preprint. In three independent scans the center position of the resonance could be reproduced within the statistical error, but slight differences in the line shape indicate systematic fluctuations of the experimental conditions which are currently analyzed in more detail (see fig. 4). We explored the resonance furthermore by searching for any change in the resonance position and line width depending on the temperature of the gas target which yields some information about collision rate and interaction mechanism between the exotic $\overline{p}He^+$atoms and the surrounding helium medium (see fig. 5). With the broad bandwidth of the high power laser we could not find any difference to the low temperature high density data which indicates that the line broadening mechanism is determined mainly by saturation broadening. To explore the natural width of the line shape in future we have to narrow the laser band width and provide lower laser light power which in turn enhances the time needed to scan

the resonance drastically (see also [9]).

Investigations on the partial initial population were possible using first one and then two lasers at the center wavelength of the resonance but triggered at different delay times with respect to the incoming $\overline{p}$ (see fig. 6). By extrapolating the signal strength on resonance to time $t = 0$, we find that the partial population of the state which we deexcite by the laser amounts to 15(1)% of the total observed metastable states. Having the first laser fixed in time and delaying the second we see an increase of the signal strength with increasing delay time of the second laser which can only be explained by feeding of the metastable state from upper levels (see fig. 7). Assuming a model where the metastable state is only repopulated by one upper level, a fit to the data shows that the upper feeding level is also metastable and populated at $t = 0$ to 9(1)%.

3.2 Influence of Hydrogen impurities on the level population and level life time

The measurements on the density dependence of the annihilation time spectra without laser (see fig. 2) indicate, that the influence of the helium in the gas target on the $\overline{p}He^+$atom is to a large extend shielded by the electron cloud surrounding the antiproton due to the Pauli exclusion. This situation is very different for any foreign atom or molecule interacting with the $\overline{p}He^+$system. By adding small impurities of hydrogen we explored the influence on the annihilation time spectra. The lifetime of the metastable states is very sensitive to even small partial pressure (see fig.8).

Using the laser to trace one particular metastable state, we can get much information about the hydrogen $\overline{p}He^+$ interaction. This method is even superior to the information we get from the lifetime spectra since one single state of the the broad initial population distribution is uniquely traced. The evaluation of the whole experimental data taken with the hydrogen impurities is still under progress. In fig. 9 preliminary data from a scan of the resonance line of the $\overline{p}He^+$system with 20 ppm hydrogen admixture in the helium gas target is shown. Since the lifetime of the metastable state is shortened by the hydrogen impurities, the signal strength is much lower at the time when we can fire the laser earliest. Within our statistical and systematic uncertainties we cannot see any change in the position or broadening due to the hydrogen impurities. The natural width of the line should be broadened due to the shorter lifetime. This cannot be seen here because of other, much larger broadening contributions as mentioned above.

References

[1] M.Iwasaki et al., *Phys. Rev. Lett.* **67** (1991) 1246.

[2] Interim report on PS205 1991 run, Interimreport 1991, PS205 collaboration (1991)

[3] Interim report on PS205 1992 run, Interimreport 1992, PS205 collaboration (1992)

[4] E. Widmann *et al.*, Proceedings of LEAP'92, Nucl.Phys.A588, (1993), 697c

[5] S.N. Nakamura *et al.*, submitted to publication in Phys. Rev. A

[6] Plan of PS205 collaboration for 1993 run, PS205 collaboration (1992)

[7] T. Yamazaki *et al.*, *Nature* **361** (1993) 238.

[8] N. Morita, K. Ohtsuki, and T. Yamazaki, Nucl. Instr. and Meth. A 330 (1993), 430

[9] Overview of 1994 experiments, PS205 collaboration, submitted to SPSLC.

List of Figures

Fig. 1: The cryostat for the cold helium gas target is surrounded by the seven shower counters (S) for detection of the annihilation products, the antiprotons entering the apparatus are counted by a thin plastic scintillator. The laser light enters through a quartz window and is reflected into itself

Fig. 2: A $\overline{p}$ annihilation lifetime in pure ^{4}He is shown. The huge peak at time t = 0 represents the 97% of the particles which annihilate prompt. Only 3% of the particles survive in metastable states.

Fig. 3: A $\overline{p}$ annihilation lifetime in pure ^{3}He is shown. The change in the long living component with respect to the ^{4}He data can be explained by the different reduced mass. The presence of the fast decaying component in the lifetime spectrum has a marked difference from the ^{4}He spectrum.

Fig. 4: The three scans of the resonance line taken at low temperature. The systematic effects leading to the significant differences in the line width are currently under investigation.

Fig. 5: A preliminary evaluation of the data from a scan of the resonance at room temperature seems to show no significant shift or change in the line width within our systematic uncertainties compared to the low temperature and higher density data which indicates that the dominant line broadening process comes from saturation broadening of the high laser power. The signal height is lower here due to different stopping distribution of the $\overline{p}$ in the He. This comes from the lower density at room temperature and leads to a different overlap of laser and particle beam.

Fig. 6: The delay time Δt_{laser} of the laser light pulse with respect to the incoming $\overline{p}$ is increased from top to bottom. The signal peak moves towards later times. The decrease of the signal strength with increasing delay time shows the depopulation of the metastable state towards lower levels. The huge peak due to prompt annihilating $\overline{p}$ has been suppressed in the online electronics.

Fig. 7: A selection of the time delay measurements with two lasers is shown for a delay time of the first laser of $\Delta t_1 = 1.8\ \mu s$ with respect to the incoming $\overline{p}$. The timing of the second laser Δt_2 varies from $\Delta t_1 + 50$ ns to $\Delta t_1 + 4.0\ \mu s$ from top to bottom. The increase at early delay times Δt_2 and later decrease of the second peak shows the repopulation of the metastable state from upper levels.

Fig. 8: The violent influence of even small hydrogen impurities on the lifetime of the metastable states in the $\overline{p}He^+$system is shown in time spectrum above. The effect that only part of the metastable states are quenched and the remaining part has a basically undisturbed lifetime is not yet fully understood.

Fig. 9: The resonance line with small admixtures of hydrogen (20 ppm) show no significant change in position of the line center or width, but the statistical uncertainty is her larger also. The broadening of the resonance line due to the shorter lifetime cannot be seen here because other broadening mechanisms are much larger.

Table 1: Overview of the measurements performed during our 1993 beam time

experiments during 1993 run	comments .	status of data
search for laser induced annihilation in the $\bar{p}He^+$system	scanned region: from 596.662 nm to 598.273 nm with 0.007 nm stepwidth, we found one resonance at 597.259(2) nm with a width of 0.018 nm and scanned also from 671.502 nm to 674.440 nm, step width: 0.02 nm using three different dyes	submitted to publication (see preprint attached)
investigation of density and temperature dependence of resonance line	effects smaller then saturation broadening of the line	under analysis
investigation of time dependence of population using 2 lasers	refilling from upper states observed	under analysis
influence of hydrogen impurities on resonance line	within errors no change observed	under analysis
influence of hydrogen impurities on the time dependence of population using 2 lasers	violent influence on lifetime of metastable state	under analysis
further study of isotope effect in ^3He and ^4He mixtures	14% change in overall lifetime due to reduced mass	under analysis

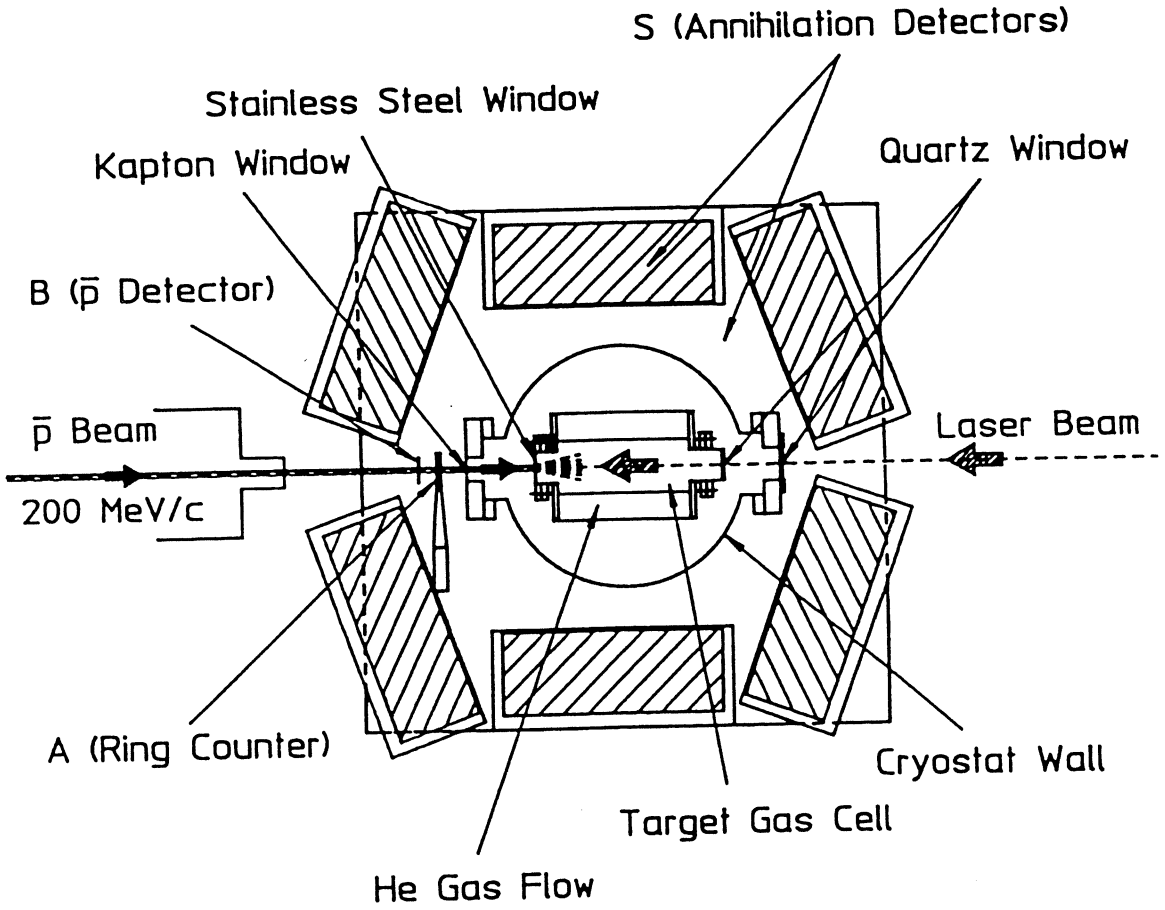

Figure 1: The cryostat for the cold helium gas target is surrounded by the seven shower counters (S) for detection of the annihilation products, the antiprotons entering the apparatus are counted by a thin plastic scintillator. The laser light enters through a quartz window and is reflected into itself.

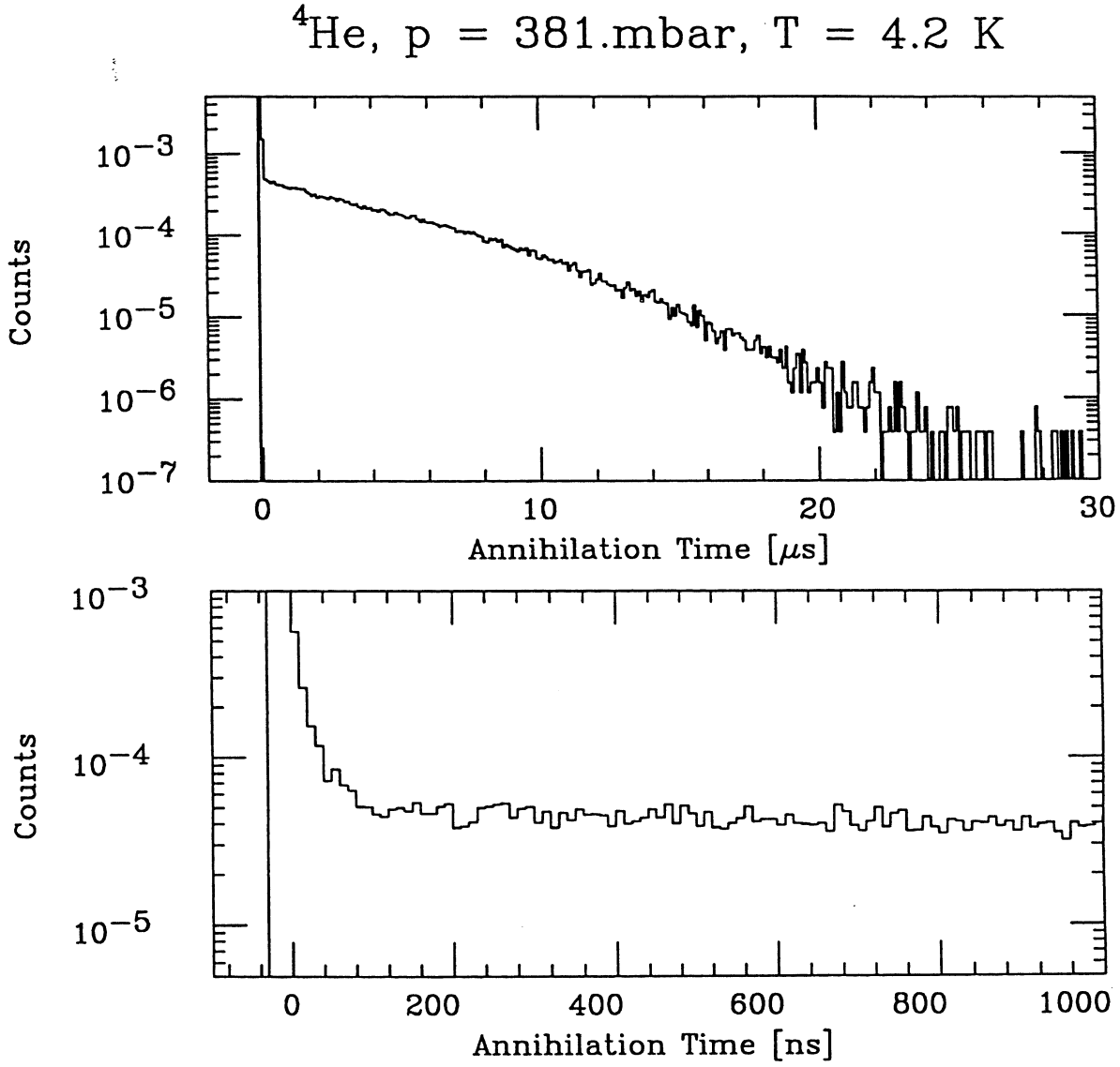

Figure 2: A $\overline{p}$ annihilation lifetime in pure ^{4}He is shown. The huge peak at time t = 0 represents the 97% of the particles which annihilate prompt. Only 3% of the particles survive in metastable states.

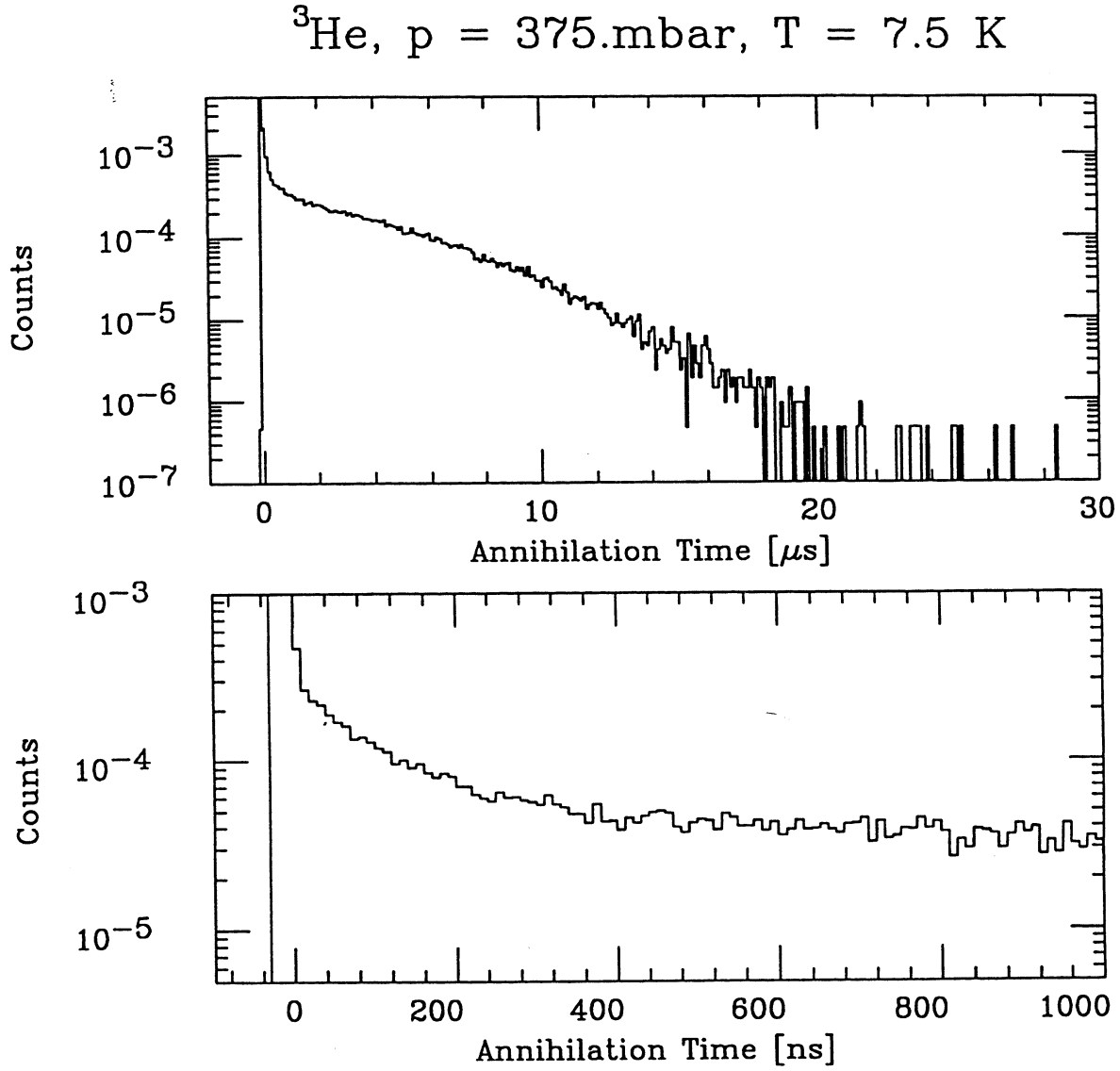

Figure 3: A $\overline{p}$ annihilation lifetime in pure ^{3}He is shown. The change in the long living component with respect to the ^{4}He data can be explained by the different reduced mass. The presence of the fast decaying component in the lifetime spectrum has a marked difference from the ^{4}He spectrum.

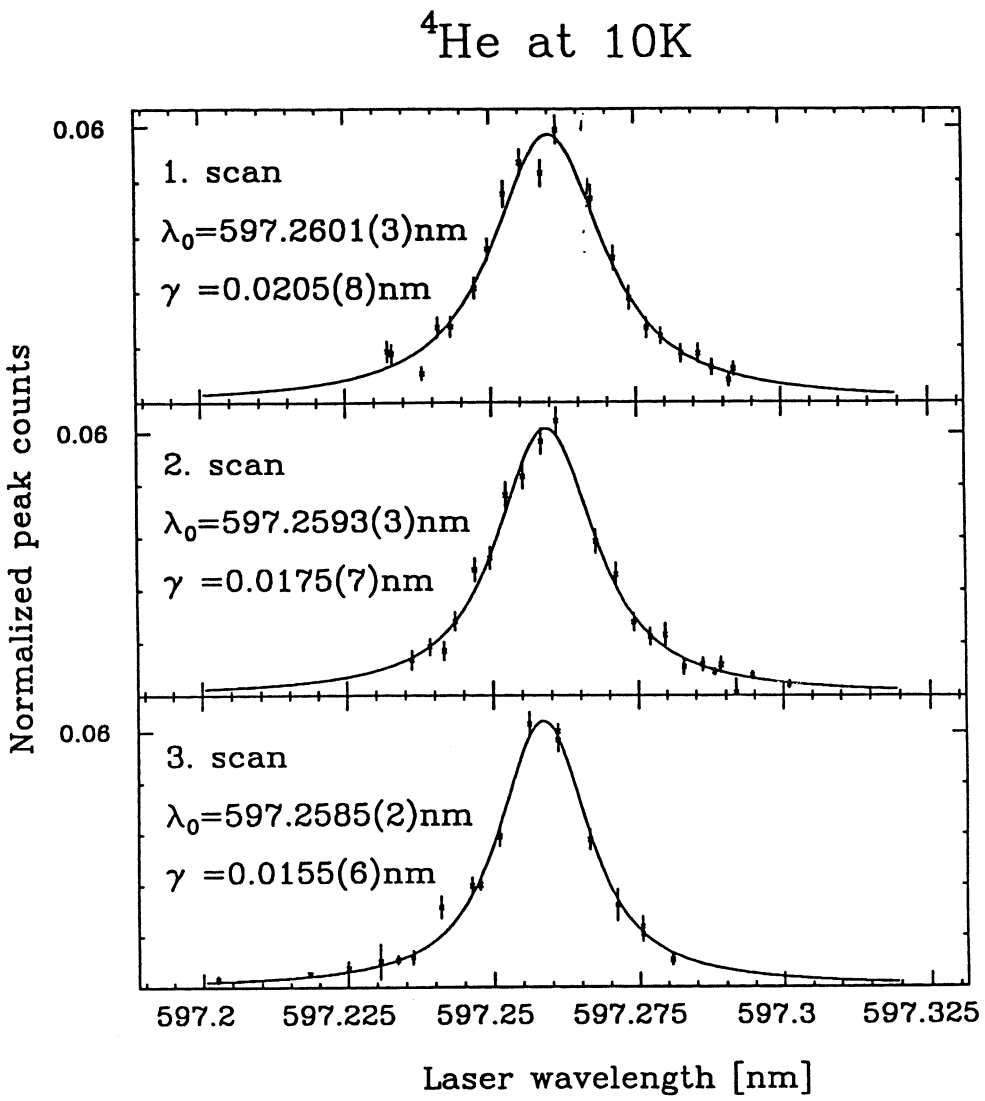

Figure 4: The three scans of the resonance line taken at low temperature. The systematic effects leading to the significant differences in the line width are currently under investigation.

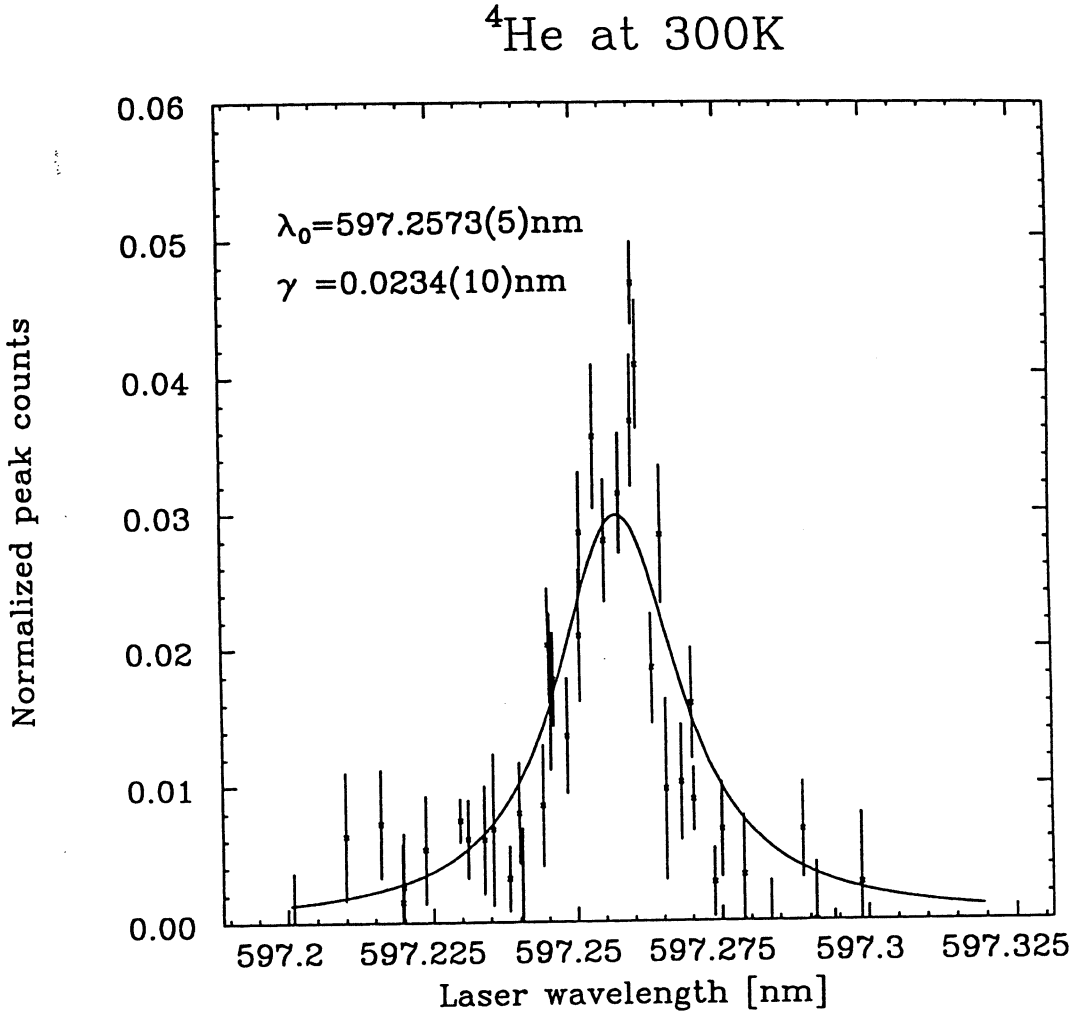

Figure 5: A preliminary evaluation of the data from a scan of the resonance at room temperature seems to show no significant shift or change in the line width within our systematic uncertainties compared to the low temperature and higher density data which indicates that the dominant line broadening process comes from saturation broadening of the high laser power. The signal height is lower here due to different stopping distribution of the $\overline{p}$ in the He. This comes from the lower density at room temperature and leads to a different overlap of laser and particle beam.

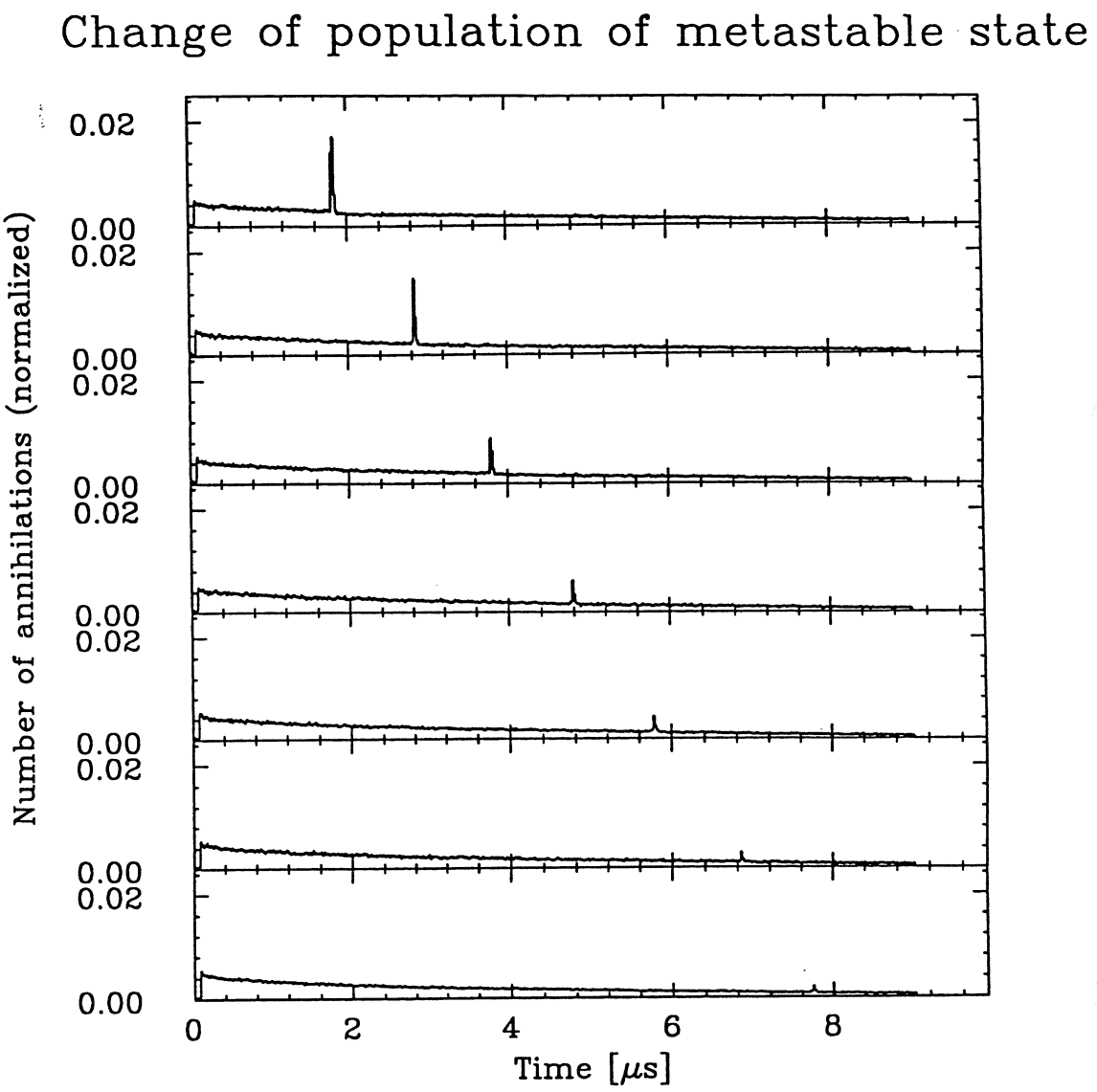

Figure 6: The delay time Δt_{laser} of the laser light pulse with respect to the incoming $\overline{\text{p}}$ is increased from top to bottom. The signal peak moves towards later times. The decrease of the signal strength with increasing delay time shows the depopulation of the metastable state towards lower levels by radiative transitions. The huge peak due to prompt annihilating $\overline{\text{p}}$ has been suppressed in the online electronics.

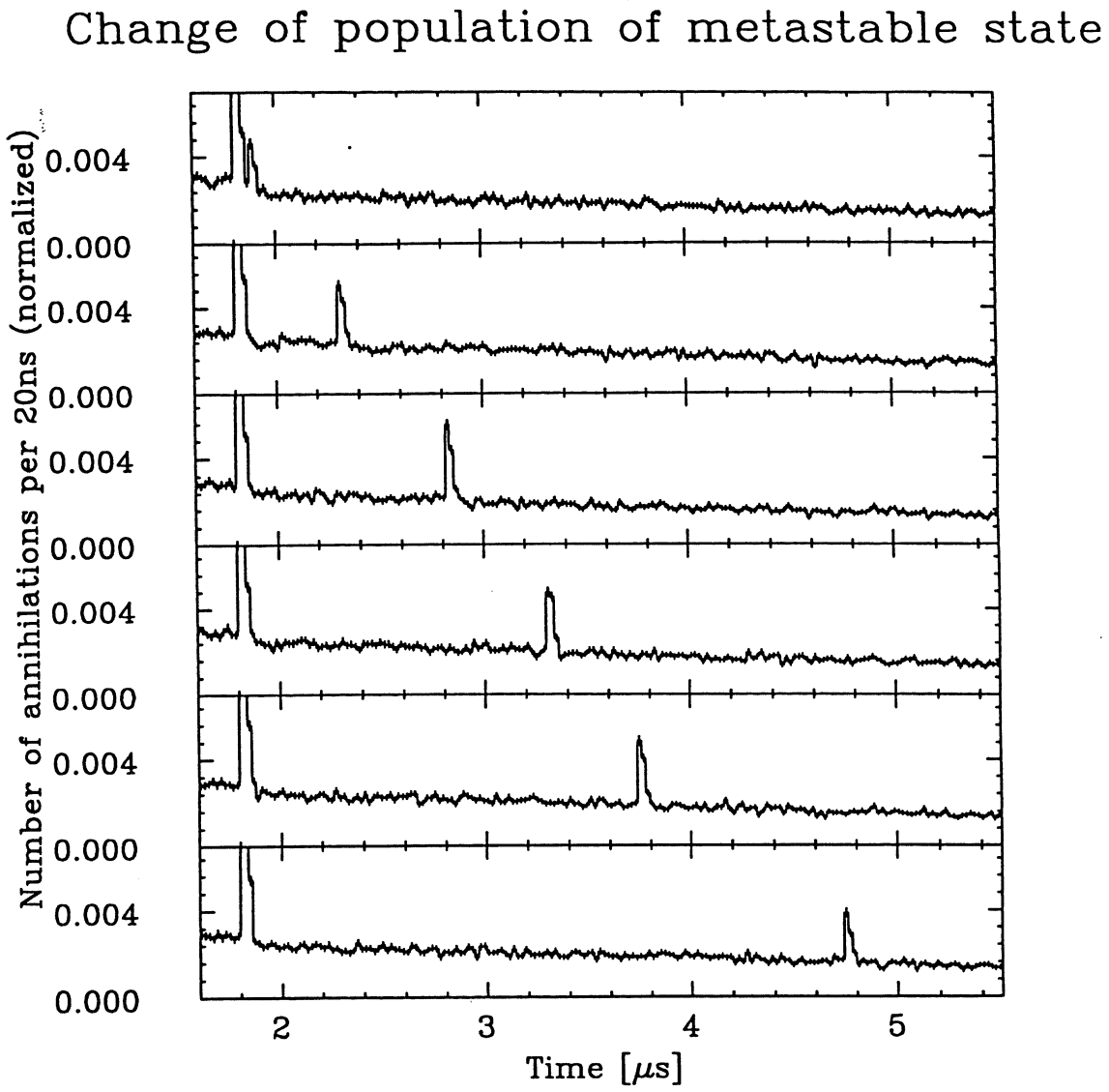

Figure 7: A selection of the time delay measurements with two lasers is shown for a delay time of the first laser of $\Delta t_1 = 1.8$ μs with respect to the incoming $\overline{\mathrm{p}}$. The timing of the second laser Δt_2 varies from $\Delta t_1 + 50$ ns to $\Delta t_1 + 4.0$ μs from top to bottom. The increase at early delay times Δt_2 and later decrease of the second peak shows the repopulation of the metastable state from upper levels by radiative transitions.

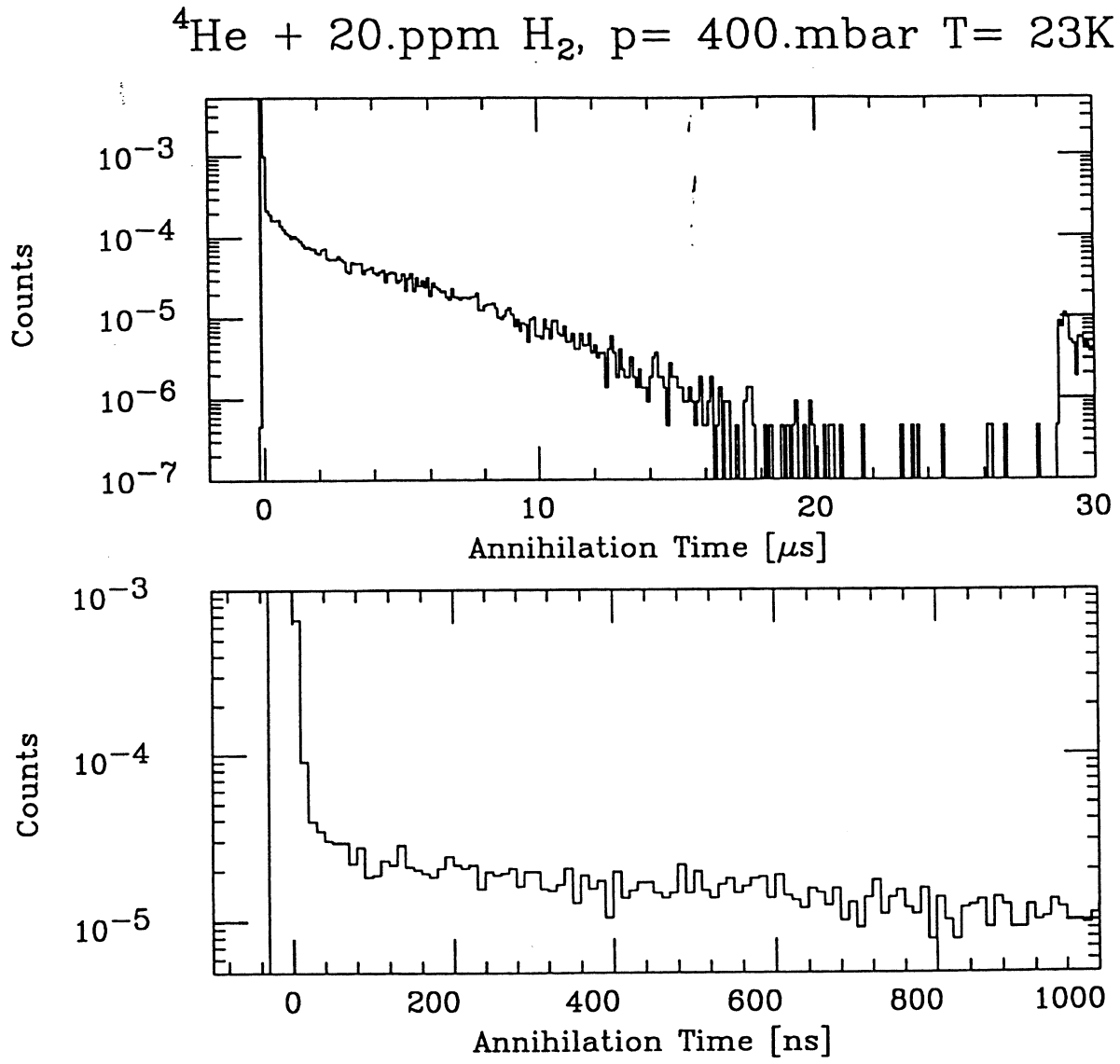

Figure 8: The violent influence of even small hydrogen impurities on the lifetime of the metastable states in the $\bar{p}He^+$system is shown in time spectrum above. The effect that only part of the metastable states are quenched and the remaining part has a basically undisturbed lifetime is not yet fully understood.

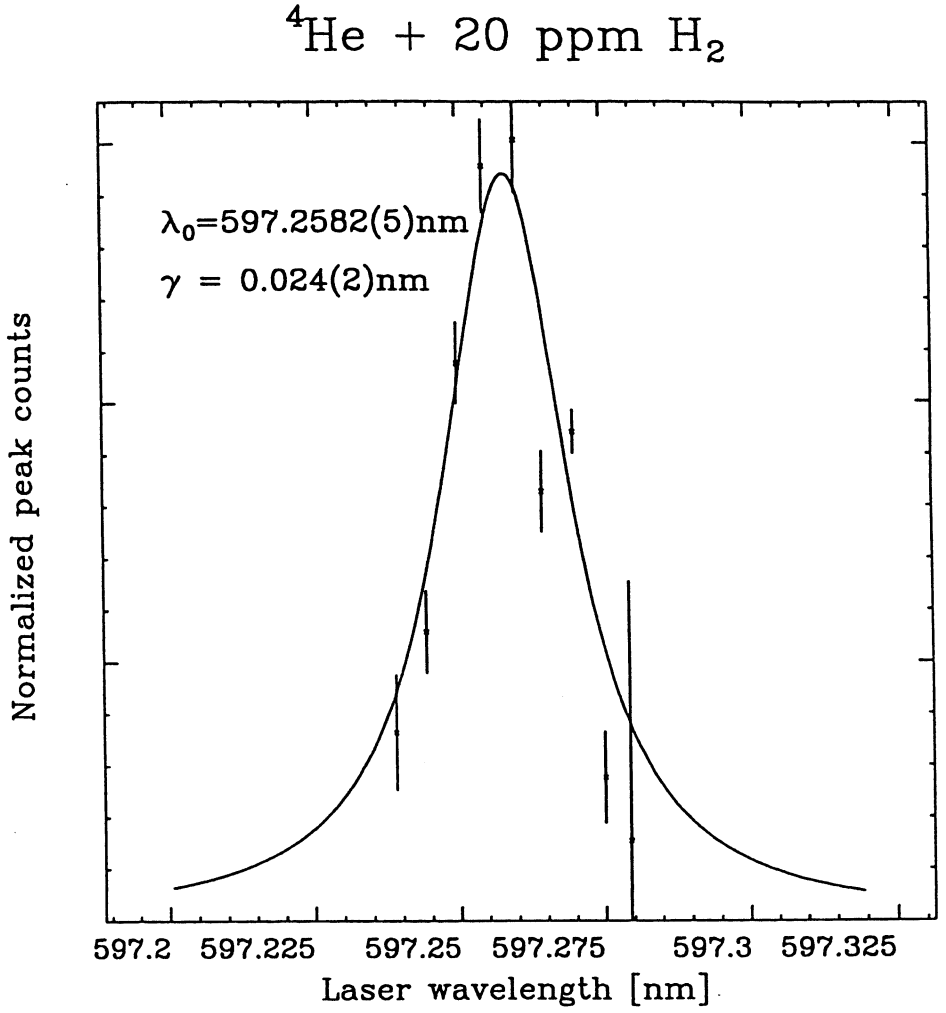

Figure 9: The resonance line with small admixtures of hydrogen (20 ppm) show no significant change in position of the line center or width, but the statistical uncertainty is here larger also. The broadening of the resonance line due to the shorter lifetime cannot be seen here because other broadening mechanisms are much larger.

FIRST OBSERVATION OF LASER-INDUCED RESONANT ANNIHILATION IN METASTABLE ANTIPROTONIC HELIUM ATOMS

N. Morita, M. Kumakura

Institute for Molecular Science, Myodaiji, Okazaki 444, Japan

T. Yamazaki, E. Widmann*, H. Masuda, I. Sugai

Institute for Nuclear Study, University of Tokyo

3-2-1 Midori-cho, Tanashi, Tokyo 188, Japan

R. S. Hayano, F. E. Maas, H. A. Torii

Department of Physics, University of Tokyo

7-3-1 Hongo, Bunkyo-ku, Tokyo 113, Japan

F. J. Hartmann, H. Daniel, T. von Egidy, B. Ketzer, W. Müller, W. Schmid

Physik-Department, Technische Universität München

D-85747 Garching, Germany

D. Horváth

KFKI Research Institute for Particle and Nuclear Physics

H-1525 Budapest, Hungary

J. Eades

CERN, CH-1211 Geneva 23, Switzerland

Submitted to Physical Review Letters

---

*Present address: CERN, CH–1211 Geneva 23, Switzerland

Abstract

We have observed the first laser-induced resonant transitions in antiprotonic helium atoms. These occur between metastable states and Auger dominated short lived states, and show that the anomalous longevity of antiprotons previously observed in helium media results from the formation of high–n high–l atomic states of $\bar{p}He^+$. The observed transition with vacuum wavelength 597.259 ± 0.002 nm is tentatively assigned to $(n, l) = (39, 35) \rightarrow (38, 34)$.

PACS 36.10.Gv, 32.80.Bx

Unusual atoms with exotic constituents such as muons and positrons have always played an important role in the development of physics. One might wonder if exotic antiprotonic atoms would show similar promise. However, theory and experiment alike have generally implied that their lifetimes ought in all cases to be very short. The entire process from capture to annihilation from high-n S-states should be over in less than a picosecond, placing antiprotonic atoms beyond the reach of many of the powerful modern techniques which have revolutionized atomic spectroscopy.

This conventional wisdom was called into question in 1991 when, in an experiment at KEK, Japan [1], a few percent of the antiprotons stopped in liquid helium were observed to have anomalously long lives, some of them annihilating up to 15 microseconds after their entry into the liquid. This intriguing effect seems peculiar to helium, and has been further studied in the gaseous, liquid and solid phases by some of the present authors using the LEAR antiproton facility at CERN. Among the wealth of new results, we found a 14 % reduction in the mean lifetime of these delayed annihilations when ^{3}He was used to stop the antiprotons instead of ^{4}He [2,3]. This is in good agreement with an estimate [4] based on a model proposed by Condo [5] and theoretically studied by Russell [6], in which the antiprotons are trapped in large-n and large-l states of neutral antiprotonic helium $\bar{p}He^+$. The initially formed states most likely have $n \sim n_0 = (M/m_e)^{1/2} \sim 38$, where M is the reduced mass of the $\bar{p}He^+$ system. Here, Auger emission is strongly suppressed, because a large jump in n and l would be necessary to provide the energy ($\sim$ 24.6 eV, the ionization energy of a helium atom) required to liberate the remaining electron. The only competitive process is then a slow radiative cascade producing $\sim$ 2 eV (visible region) photons. Furthermore, the presence of an electron in the $\bar{p}He^+$ atom during this cascade strongly suppresses collisional quenching of the metastability by a) ensuring the atom's neutrality, b) removing the l-degeneracy of the $\bar{p}$ atomic levels and c) providing a Pauli-repulsion effect. The isotope effect alone could not however be unequivocally attributed to the formation of particular atomic structures. It was clear that a more informative and conclusive experiment would be to induce resonant transitions between internal energy levels of the exotic atom in question by laser irradiation.

In the present letter we report results on the first laser spectroscopy experiment ever done with antiprotonic exotic atoms, and establish the large (n,l) states of neutral $\bar{p}He^+$ as the source of the observed metastability. Our method, described in detail in [7], is to use a high-power dye laser pulse to stimulate resonant transitions between metastable/non-metastable pairs of states differing by one unit in l. After Auger deexcitation of the newly populated short lived member to a $\bar{p}He^{++}$ ion, annihilation should follow within picoseconds via Stark mixing, and produce a sharp peak in the annihilation-time spectrum at the time the laser pulse is applied. Recent theoretical calculations by Ohtsuki [7,8] of $\bar{p}He^+$ energy levels, their populations, and their Auger and radiative rates were used as a guide in searching for suitable transitions. In the present search we concentrated on the candidate transition $(n,l) = (39,35) \rightarrow (38,34)$ whose vacuum wavelength is expected to be around 598 nm (Fig. 1). This method is clearly superior to that of stimulating transitions between two metastable levels, which would change the annihilation-time spectrum only slightly.

The 200 MeV/c $\bar{p}$ beam from the LEAR storage ring used in these experiments, was extracted in an 80 minute long spill at an intensity of some 10^4 /s. The beam traversed a 0.5 mm thick plastic scintillation counter (B in Fig. 2) before entering a target-gas chamber. We used low temperature helium gas at a pressure between 0.7 and 1 bar, since we have found that these conditions provide the best environment for studying the metastability [9]. The chamber and its contents were maintained at 5–10 K by cold helium gas (evaporated from a separate liquid helium reservoir) which flowed around the chamber walls. The small emittance (10π mm mrad in both directions) and momentum bite (0.1 %) of the LEAR beam meant that we could achieve a stopping volume of about $1 \times 1 \times 5$ cm^3 in helium at these temperatures and pressures. Light from the B counter edges was viewed by two phototubes operated in coincidence, while light emerging from its surface was seen by a CCD image-intensified camera with its axis at 45 degrees to the beam axis. This provided us with a continuously visible image of the beam spot which was used to maintain the alignment of the antiproton beam with the laser beam. The latter entered the target chamber through a downstream quartz window, and left it after reflection from the highly polished inner surface

of the antiproton beam entrance window.

The lasers were to be ignited by all events for which no prompt annihilation had been detected. These occurred with a random time distribution and at a rate ($\sim$ 400 /s) close to the maximum laser repetition rate. We therefore had to make sure that the much more numerous prompt annihilations were vetoed with very high efficiency, since even a small undetected prompt fraction would generate many spurious triggers. For this purpose the helium target was surrounded by stacks of interleaved lead plates and plastic scintillators ("shower counters", labelled S in Fig. 2) which were designed to detect both charged and neutral pions from $\bar{p}$ annihilations with high efficiency. The S counter stacks had a thickness of about 5 radiation lengths and were estimated to have an overall efficiency of about 99.7 % for $\bar{p}$ annihilation events. In the laser experiments, any event in which an S signal was received within 100 ns of a B signal was discarded as a prompt annihilation. If no such "prompt" S signal was received, we assumed that a metastable $\bar{p}He^+$ atom was present in the gas, and after a suitable delay allowed the B counter pulse to ignite the laser. Our method of obtaining undistorted and background-free $\bar{p}$ annihilation time spectra is described in detail in [3]. In the present laser runs we recorded delayed annihilations occurring in the 10 μs following the $\bar{p}$ arrival time. Control events without laser irradiation were accumulated during the laser dead time of 2.5 ms. We searched the region of the expected resonance by scanning the wavelength step by step, the typical run time for one wavelength point being about 20 minutes.

Our laser system consisted of two pulsed dye lasers (Lambda Physik LPD3002) pumped at 308 nm by XeCl excimer lasers (Lambda Physik LPX240i). In the wavelength range of the present experiment (595–600 nm) the dye used was Rhodamine 6G dissolved in methanol. The two lasers could be scanned in different wavelength regions simultaneously in order to search for the resonance more quickly. The laser beams were expanded to about 15 mm in diameter to cover the transverse $\bar{p}$ stopping distribution and were merged before they entered the target chamber. Their wavelengths were measured with pulse-mode wavemeters (Burleigh WA4500), the calibration of which was periodically verified against opto-galvanic

signals from an Argon discharge cell, using an air gap etalon. The energy in each dye laser pulse was measured by PIN photodiodes, the values obtained being frequently calibrated against a calorimeter (Scientech AC2501). The excimer pulse energies were also recorded pulse by pulse using biplanar detectors and were calibrated against another calorimeter (Scientech AC50UV). Typical excimer pulse energies were in the region 80–140 mJ, and produced dye laser pulses of energy 3-5 mJ.

In Fig. 3 (left), we show a series of annihilation–time spectra obtained at vacuum wavelengths near 597.2 nm. The delay in igniting the laser after receiving a 'no prompt annihilation' B signal was in each case 1.8 μs (the minimum we could achieve with the present setup). As the wavelength passes through the value 597.26 nm, a sharp peak appears in the spectrum, indicating forced annihilation via the mechanism described above. An enlarged view of the peak near the wavelength of maximum excitation is given in Fig. 3 (upper right). The peak profile showed an exponential decay with a time constant of 15 ± 1 ns, which reflects the lifetime of the Auger-dominated short lived state (although it also depends on the laser power and pulse profile). The integrated number of annihilation counts over the peak corresponds to the population of the initial metastable state at the laser ignition time. Even though this particular state contains only a fraction of the total metastable-state population, the laser-induced spike shows a striking peak/background ratio ($\sim$ 10:1 on resonance). No other resonances were found over the ranges of vacuum wavelength scanned (from 594.152 to 594.370 and from 596.662 to 598.273 nm).

The resonance curve of Fig. 3 (lower right) displays the background subtracted number of delayed annihilations in the peak region normalized to their total number, plotted against wavelength. When the laser bandwidth of 0.007 nm (assumed Gaussian) has been deconvoluted, we find a mean vacuum wavelength of 597.259 ± 0.002 nm and a FWHM width of 0.018 nm. Minor perturbations in the antiproton beam position during the scan could not be followed in the CCD image and could give rise to small systematic effects. Taking these as well as systematic uncertainties in the wavelength calibration into account, we have assigned for the moment the conservative error given above to the resonance position. The width

of the resonance line is larger than the laser bandwidth (0.007 nm), presumably because of collisional and power broadening. No measurement was made of the pressure shift.

The observed resonance wavelength can be compared with the theoretical calculations for the transition $(n = 39, l = 35) \rightarrow (n = 38, l = 34)$ in $\bar{p}He^+$. The calculation based on the molecular approach (Born-Oppenheimer approximation) by Shimamura [10] gives 598.01 nm, while Greenland and Thürwächter [11] predict 598.10 nm in a similar calculation. The configuration mixing calculation by Ohtsuki [8] yields 597.11 nm. Considering that these calculations did not aim to equal the precision we achieved in our laser spectroscopy measurement, it is fair to say that the experimental value is in good agreement with them all. Since the transition energy depends strongly on n, we can assign it uniquely to $n = 39 \rightarrow 38$. On the other hand, the transition energies for $(39, l) \rightarrow (38, l-1)$ are nearly degenerate, and we cannot determine l from the resonance energy alone. The present assignment of the resonant transition to $(39, 35) \rightarrow (38, 34)$ is based on the theoretical estimate by Ohtsuki [7,8] of the boundary between the radiation-dominated long lived states and the Auger-dominated short lived states, and thus is somewhat model dependent. From the observed 15 ± 1 ns decay time of the peak, the lifetime of the Auger-dominated state has been estimated to be $7ns$, which is in remarkable agreement with the theoretical value [7,8] . The integrated number of counts in the observed peak indicates that the partial population of the parent state at 1.8 μs is at least 6 % of the total metastable fraction, again consistent with expectations [7,8].

In summary, we have carried out the first laser spectroscopy experiment on antiprotonic exotic atoms and demonstrated that the longevity against annihilation shown by some 3 % of all antiprotons stopped in helium is due to the formation of $\bar{p}He^+$ atoms with large n and l. The transition energy has been determined precisely, and the lifetime of the Auger dominated state and the partial population of the parent metastable state have been deduced. All this "microscopic" information supports theoretical predictions of the characteristics of $\bar{p}He^+$ atoms. We expect in the future to use our laser tools to study the formation, structure and reactions of this new atomic species in more detail.

We are indebted to the LEAR and PS staff at CERN for their tireless dedication to providing us with our antiproton beam, to A.D. Donnachie and P. Darriulat for encouragement, to K. Ohtsuki for many valuable discussions and theoretical results and to T. Morimoto for invaluable help in designing the experimental setup. The present work is supported by the Grants-in-Aid for Specially Promoted Research and for International Scientific Research of the Japanese Ministry of Education, Science and Culture, the Japan Society for the Promotion of Science (JSPS) and the Bundesministerium für Forschung und Technologie. E. W. and F. E. M. acknowledge the receipt of JSPS and INOUE fellowships, respectively.

REFERENCES

[1] M. Iwasaki, S. N. Nakamura, K. Shigaki, Y. Shimizu, H. Tamura, T. Ishikawa, R. S. Hayano, E. Takada, E. Widmann, H. Outa, M. Aoki, P. Kitching and T. Yamazaki, Phys. Rev. Lett. **67**, 1246 (1991).

[2] T. Yamazaki, E. Widmann, R. S. Hayano, M. Iwasaki, S. N. Nakamura, K. Shigaki, F. J. Hartmann, H. Daniel, T. von Egidy, P. Hofmann, Y.–S. Kim and J. Eades, Nature **361**, 238 (1993).

[3] S.N. Nakamura, R.S. Hayano, M. Iwasaki, K. Shigaki, E. Widmann, T. Yamazaki, H. Daniel, T. von Egidy, F.J. Hartmann, P. Hofmann, Y.-S. Kim and J. Eades, *submitted to Phys. Rev. A.*

[4] T. Yamazaki and K. Ohtsuki, Phys. Rev. A **45**, 7782 (1992).

[5] G. T. Condo, Phys. Lett. **9**, 65 (1964).

[6] J. E. Russell, Phys. Rev. Lett. **23**, 63 (1969); Phys. Rev. **188**, 187 (1969); Phys. Rev. A **1**, 721, 735, 742 (1970).

[7] N. Morita, K. Ohtsuki and T. Yamazaki, Nucl. Instr. Meth. A **330**, 439 (1993).

[8] K. Ohtsuki, private communication (1993).

[9] E. Widmann, H. Daniel, J. Eades, T. von Egidy, F.J. Hartmann, R.S. Hayano, W. Higemoto, J. Hoffmann, T.M. Ito, Y. Ito, M. Iwasaki, A. Kawachi, N. Morita, S.N. Nakamura, N. Nishida, W. Schmid, I. Sugai, H. Tamura and T. Yamazaki, Nucl Phys. **A558**, 679c (1993).

[10] I. Shimamura, Phys. Rev. A **46**, 3776 (1992); private communication (1993).

[11] P.T. Greenland and R. Thürwächter, Hyperfine Interactions 76, 355 (1993); P.T. Greenland, private communication (1993).

FIGURES

FIG. 1. Relevant energy levels versus orbital angular momentum of metastable antiprotonic helium atom $\bar{p}He^+$ calculated by Ohtsuki [7,8]. The levels indicated by bold lines have long lifetimes, while those indicated by broken lines are Auger-dominated with short lifetimes. The calculated Auger rates (upper number) and radiative rates (lower number) per second are attached to each level, the number in parentheses being the power of 10. Possible laser-induced transitions for forced annihilation are indicated by arrows, with the present search candidate shown by a bold arrow.

FIG. 2. Experimental setup. 200 MeV/c $\bar{p}$'s, passing through a beam counter (B) and the hole in a ring counter (A), are stopped in a target chamber containing helium, which is cooled to 5-10 K at 0.7-1 bar. Seven $\bar{p}$ annihilation counters (S, 6 sides and 1 bottom) are located around the target. Two laser beams enter the target chamber through quartz windows from the direction opposite to the $\bar{p}$ beam.

FIG. 3. (Left) Observed time spectra of delayed annihilation of antiprotons with laser irradiation of various vacuum wavelengths near 598.2 nm, normalized to the total delayed component. Spikes due to forced annihilation through the resonance transitions are seen at 1.8 μs. (Upper right) Enlarged time profile of the resonance spike. A damping shape with a time constant of 15 ± 1 ns is observed. (Lower right) Normalized peak count versus vacuum wavelength in the resonance region, showing a central wavelength 597.259 ± 0.002 and a FWHM 0.018 nm.

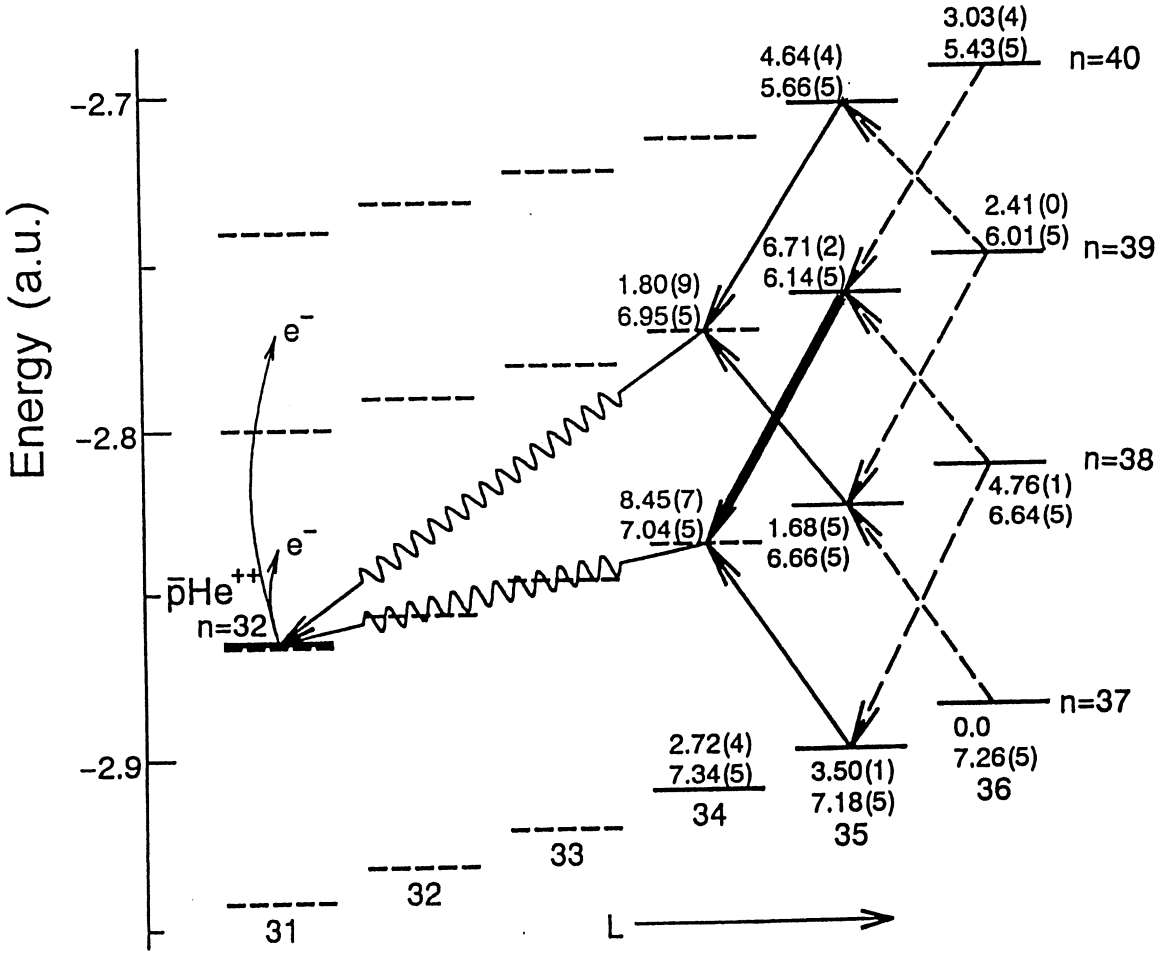
Energy (a.u.)
-2.7
-2.8
-2.9
e⁻
e⁻
p̄He⁺⁺
n=32
4.64(4)
5.66(5)
3.03(4)
5.43(5)
n=40
2.41(0)
6.01(5)
n=39
6.71(2)
6.14(5)
1.80(9)
6.95(5)
n=38
4.76(1)
6.64(5)
8.45(7)
7.04(5)
1.68(5)
6.66(5)
n=37
0.0
7.26(5)
36
2.72(4)
7.34(5)
34
3.50(1)
7.18(5)
35
33
32
31
L

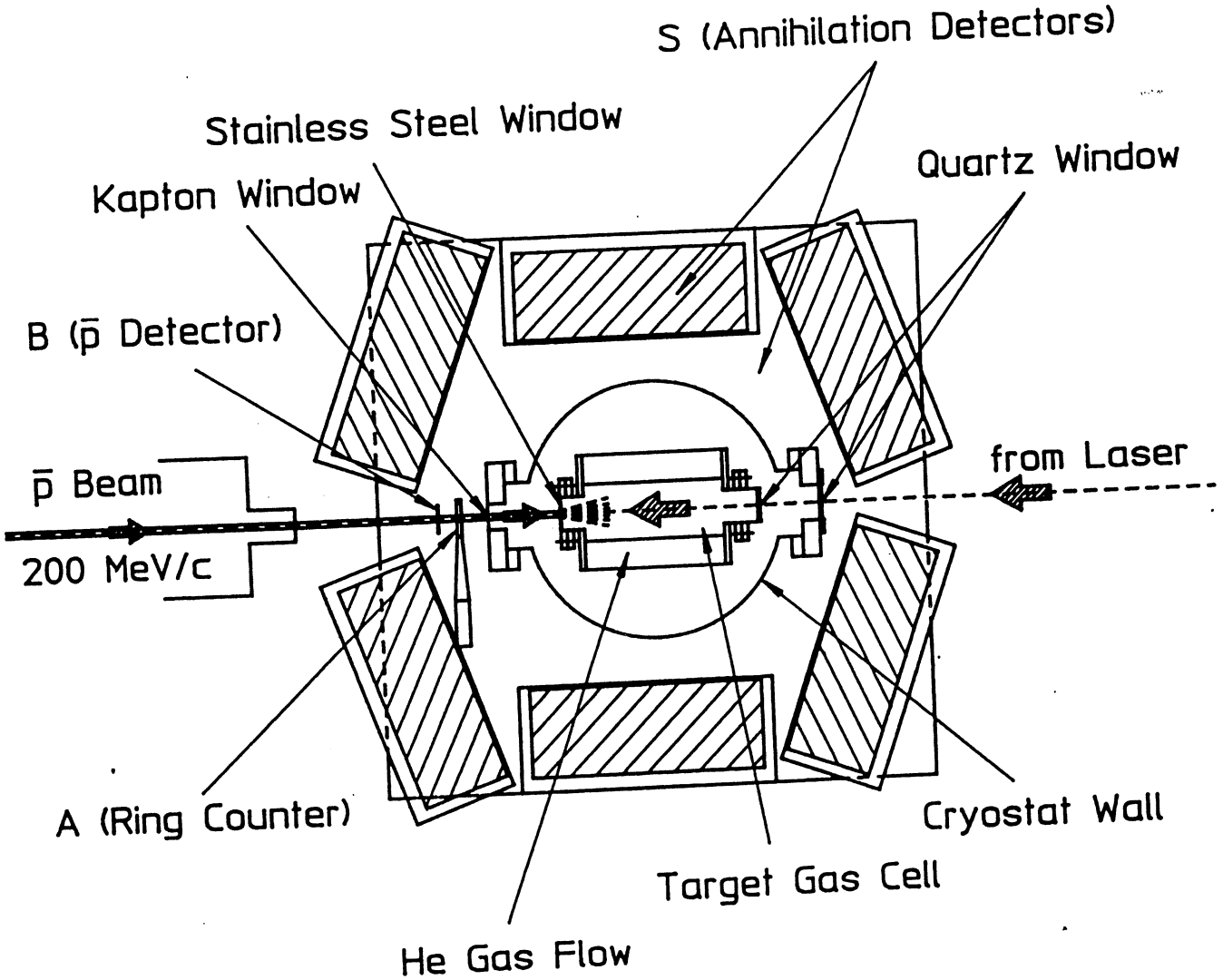
S (Annihilation Detectors)
Stainless Steel Window
Quartz Window
Kapton Window
B ($\bar{p}$ Detector)
$\bar{p}$ Beam
200 MeV/c
from Laser
A (Ring Counter)
Cryostat Wall
Target Gas Cell
He Gas Flow

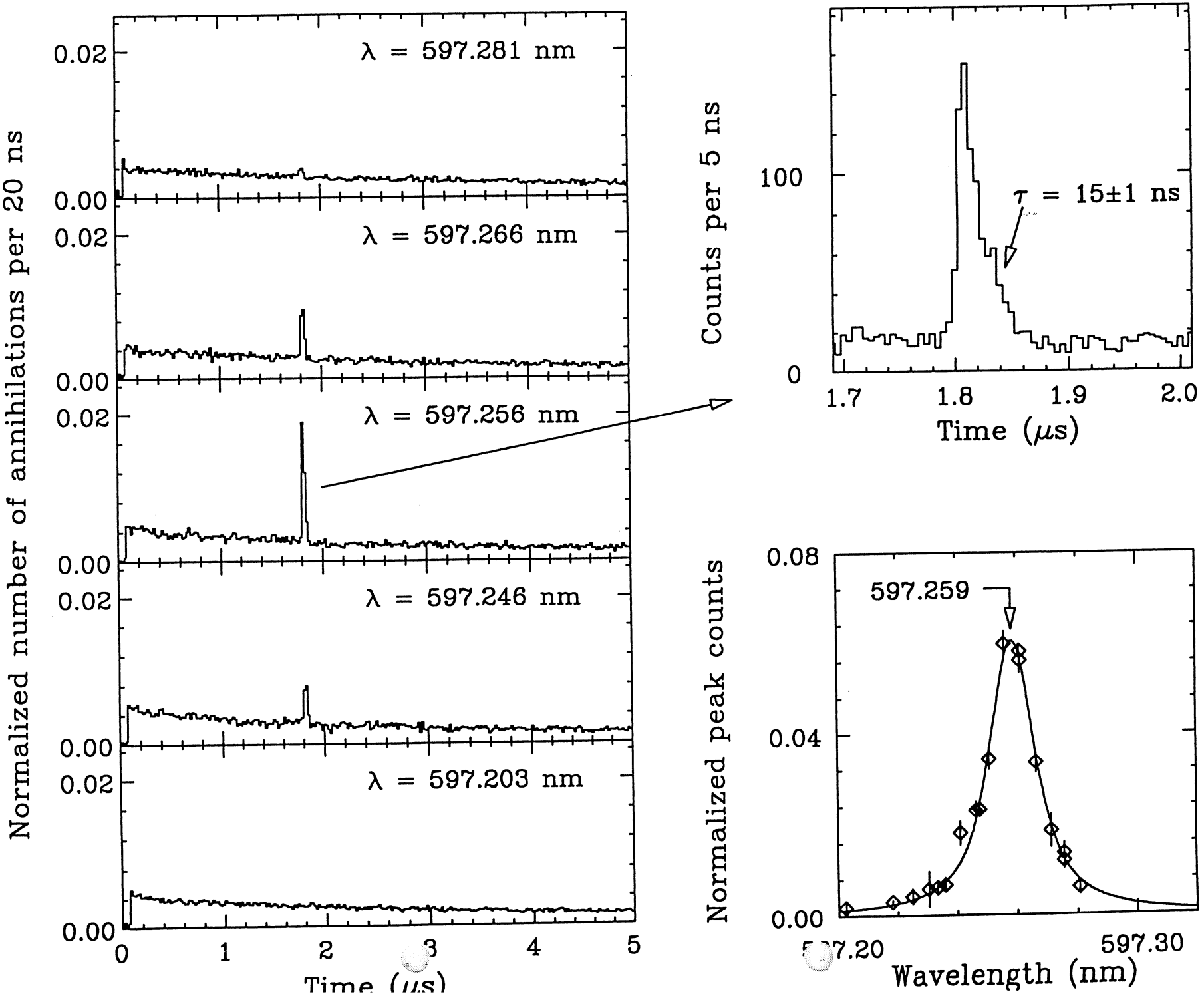
λ = 597.281 nm
λ = 597.266 nm
λ = 597.256 nm
λ = 597.246 nm
λ = 597.203 nm
0.02
0.00
Normalized number of annihilations per 20 ns
0
1
2
3
4
5
Time (μs)
Counts per 5 ns
100
0
τ = 15±1 ns
1.7
1.8
1.9
2.0
Time (μs)
Normalized peak counts
0.08
0.04
0.00
597.259
597.20
597.30
Wavelength (nm)